The Chemical Oxidation and Immobilization of Arsenic and Antimony in Simulated AMD in Karst Areas

Jian Zhu[1,2,3] [ID] · Peng Liao[3,4] · Peng Zhang[3]

Abstract

The widely distributed carbonate rock in karst areas can neutralize AMD, increase pH and promote Fe(II) oxidation, which produce reactive oxidation species (ROS) and iron (hydr)oxides. (ROS) and iron (hydr)oxides can facilitate oxidation and immobilization of As and Sb. The flow, pH and Fe(II) concentration of AMD may affect oxidation or immobilization of As/Sb via affecting of Fe(II) oxidation in AMD. This study investigated the influence of Fe(II) oxidation on the transfer and transformation of As/Sb in simulated AMD induced by carbonate. Low flow and high pH were beneficial for Fe(II) oxidation to produce ROS/Fe(IV) and iron (hydr)oxides to oxidize As(III)/Sb(III). Fe(II) concentration (100–500 mg/L) had negligible influence on oxidation and sediment of As(III)/Sb(III). With increase of reaction time, difference in As(III)/Sb(III), total As/ Sb concentrations between different flow distances were decreasing.

Keywords Arsenic · Antimony · Fe(II) · Transfer · Transformation · Karst areas

Acid mine drainage (AMD) causes serious environmental pollution around the world because it contains high concentration Fe(II) and trace toxic metals (Arnold et al. 2011). As and Sb are widely distributed in AMD, their concentraitions up to 850,000 µg/L (Cheng et al. 2009) and 39,160 µg/L (Zhou et al. 2017). Due to the high toxicity of As and Sb, they are cosidered a priority pollutant by the Environmental Protection Agency of the United States and the Council of the European Communities (Kong et al. 2015). As and Sb are mainly composed of As(III) and As(V), Sb(III) and Sb(V) respectively in AMD. As(III)/Sb(III) are more acutely toxic than As(V)/Sb(V), and the adsorption by iron (hydr) oxides weaker than As(V)/Sb(V) at acid condition (Cheng et al. 2009; Dixit and Hering 2003). As(III) or Sb(III) are major species when AMD flow from outlet (Casiot et al. 2003). As(III)/Sb(III) can be oxidized by abiotic and biotic factors, and mainly precipitate to sediment via adsorption, precipitation and co-precipitation by iron (hydr)oxides (Cheng et al. 2009; Kiran et al. 2017; Razo et al. 2004).

Karst areas occupy 10–15% of global land area (Ford and Williams 2013) and its typical characteristic is rich of carbonate. AMD also distributes widely in karst areas, e.g., Dongfeng antimony ore in Dushan county of China. Carbonate can accelerate Fe(II) oxidation via improving the pH of AMD to produce reactive oxidants (ROS) and Fe(IV) which can oxidize rapidly As(III)/Sb(III) in karst area in dark (Zhu et al. 2017). At the same time, the iron (hydr)oxides produced from Fe(II) oxidation induced by carbonate can co-precipitate As/Sb. The flow, pH and Fe(II) concentration of AMD may influence oxidation or immobilization of As/Sb in AMD.

Therefore, this study aims to check the the factors controlling the chemical oxidation and removal of As/Sb from AMD in karst areas. To achieve this goal, a bench -scale reactors were filled with quarts sand and carbonate rock, and supplied with simulated AMD. As, Sb and Fe species in aqueous and solid were determined.

✉ Jian Zhu
  Jzhu@gzu.edu.cn

1 College of Resource and Environmental Engineering, Guizhou University, Guiyang 550025, People's Republic of China

2 Key Laboratory of Karst Georesources and Environment, Ministry of Education, Guizhou University, Guiyang 550025, People's Republic of China

3 State Key Laboratory of Biogeology and Environmental Geology, China University of Geosciences, 388 Lumo Road, Wuhan 430074, People's Republic of China

4 State Key Laboratory of Environmental Geochemistry, InstituteofEochemistry, Chinese Academy of Sciences, Guiyang 550081, People's Republic of China

Materials and Methods

Section S1 of Supporting Information.

Section S2 of Supporting Information.

Three experiments referred flow chemical oxidation experiments were conducted in the reactor. The sand in reactor was soaked with deionized water for 1 h before continuous flow experiments. To evaluate the influence of flow rate on As/Sb oxidation, the flow rates of simulated AMD (500 µg/L As(III), 500 µg/L Sb(III), 500 mg/L Fe(II), pH 3) were fixed at 5, 15 and 30 mL/min, separately. The experiment was operated in natural sunlight irradiation at 26.3°C. To evaluate the influence of pH on As/Sb oxidation, simulated AMD (500 µg/L As(III), 500 µg/L Sb(III), 500 mg/L Fe(II)) were fixed at pH 2, 3 or 4, separately. AMD was pumped at 15 mL/min in natural sunlight irradiation at 24.1°C. To evaluate the influence of Fe(II) concentration on As/Sb oxidation, Fe(II) concentrations of simulated AMD (500 µg/L As(III), 500 µg/L Sb(III), pH 3) were fixed at 100, 300, 500 mg/L, separately. AMD was pumped at 15 mL/min in natural sunlight irradiation at 23.0°C. To explore As/Sb distribution in sediment with increase of time, simulated AMD (500 µg/L As(III), 500 µg/L Sb(III), 500 mg/L Fe(II), pH 3) was pumped at 15 ml/min in natural sunlight irradiation at 25.3°C. In order to evaluate the contribution of ·OH and Fe(IV) produced from Fe(II) oxidation on As(III)/Sb(III) oxidation, simulated AMD (500 µg/L As(III), 500 µg/L Sb(III), 500 mg/L Fe(II), pH 3) was pumped at 15 mL/min in natural sunlight irradiation at 25.0°C, and 100 mM 2-propanol for scavenging ·OH scavenger (Keenan and Sedlak 2008a), 1 M ethanol for scavenging ·OH and Fe(IV) were added into simulated AMD for comparison, separately (Shi et al. 2014).At predetermined time intervals, the suspension was withdrawn for analysis of pH, As or Sb species and Fe(II) contents. For analysis of dissolved As or Sb species, the samples were filtered through 0.45 µm membranes and acidified by 1.2 M HCl. For analysis of total As, Sb and Fe(II), the suspensions were digested by 2 M HCl for 20 h (Jeon et al. 2003).

The oxygenation experiments were performed in a 500 mL bottles at the room temperature (25 ± 1°C). 0.347 g $CaCO_3$ powder (1.39 g/L) was added to 250 mL simulated AMD (500 mg/L Fe(II), pH 3) to start the oxygenation process at 560 rpm using a Teflon-coated magnetic bar. The bottles were wrapped by silver paper to avoid light, and open to air by several small holes. High-purity N_2 (99.999%) was introduced into the bottles to purge O_2 in suspension and bottle for 30 min after oxygenation experiments in 1, 2 or 12 h, separately. 500 µg/L As(III) and 500 µg/L Sb(III) were added into suspension in an anoxic glovebox (92% N_2 and 8% H_2, 0 ppm O_2,

COY, USA). At predetermined time intervals, the suspension was withdraw for analysis of pH, As, Sb species and Fe(II) contents. The oxygenation experiments were carried out in duplicate.

Section S3 of Supporting Information.

Results and Discussion

The AMD flow AMD was influenced by rainfall. The Fig. 1 shown that dissolved total As and Sb concentration increased with AMD flow (Fig. 1a, c). That suggested that greater flow of AMD contribute to transport of As and Sb for a long distance. The more H^+ could react with carbonate in limestone with large AMD flow, that decreased rise of AMD pH (Fig. S2a). Low pH suppressed oxidation of As(III),Sb(III) or Fe(II). Production of iron oxyhydroxide which could adsorb As and Sb (Cheng et al. 2009; Guo et al. 2014) reduced due to slow oxidation rate of Fe(II) in low pH (Stumm and Lee 1961) (Fig. S2b), so dissloved total As and Sb concentrations increased with AMD flow (Fig. 1a, c).

The ROS and Fe(IV) (Zhu et al. 2017) could be produced from oxygenation of simulated AMD with contact of carbonate could oxidze As(III) (Dutta et al. 2005; Hug and Leupin 2003) and Sb(III) (Kong et al. 2015), so dissolved As(III) or Sb(III) concentrations decreased (Fig. 1b, d). Meamwhile, iron oxyhydroxide produced from Fe(II) oxidation adsorbed As(III) and Sb(III) during the process, that lead As(III)/Sb(III) concentrations decreased (Fig. 1b, d).

Small flow of AMD contributed Fe(II) oxidation by O_2 (Fig. S2b) to produce more ROS and Fe(IV) to oxidize As(III)/Sb(III). So, dissoved As(III) and Sb(III) concentrations decreased with decrease of flow of AMD (Fig. 1b, d). Carbonate was consumed or covered by iron (hydr)oxides with increased of reaction time. The decrease of pH of AMD inhibited Fe(II) oxidation to produce ROS and Fe(IV) to oxidize As(III) and Sb(III), As(III)/Sb(III) concentrations were increasing (Fig. 1b, d). The result that dissolved Sb(III) concentration was lower than dissolved As(III) concentration in AMD (Fig. 1b, d) showed that Sb(III) was more easily oxidized than As(III), the oxidation mechanism was discussed in 3.5.

The pH of AMD increased with flow of AMD on account of neutralization of carbonate. High pH acclerated Fe(II) oxidation (Fig. S3b) to produce iron (hydr)oxide, which can adsorb quickly As and Sb. So, total dissolved As and Sb concentrations decreased with increase of pH (Fig. 2a, c). The pH increased to 5–6 after the reaction of limestone with AMD at pH 3–4. An appropriate pH (5−6) was required for the moderate oxidation of Fe(II) toproduce maximum ROS such ·OH (Zhu et al. 2017), so As(III) and Sb(III) were oxidized quickly (Fig. 2b, d). pH of AMD was low (pH < 3.5)
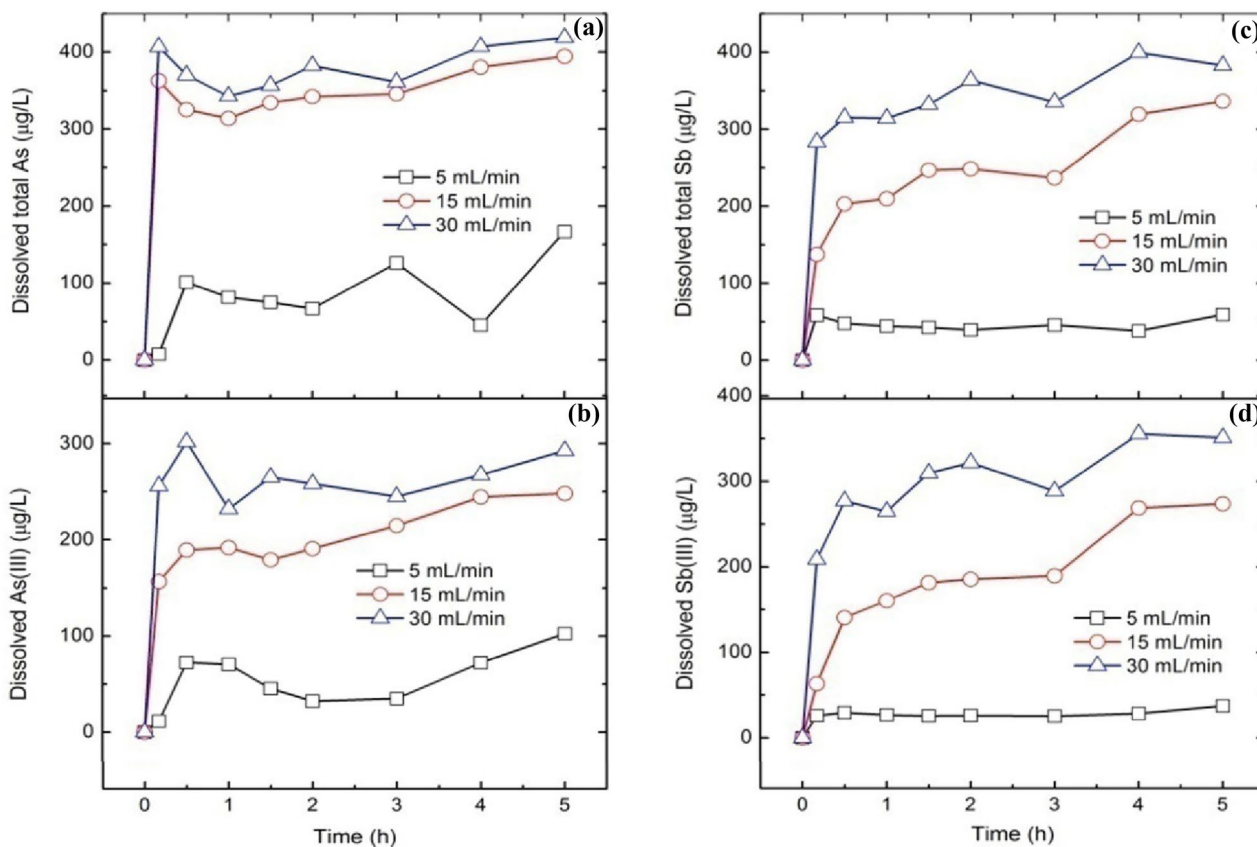
Fig. 1 The concentrations of **a** dissolved total As, **b** dissolved As(III), **c** dissolved total Sb and **d** dissolved Sb(III) in AMD in the third step outlet

after the reaction of limestone with AMD at pH 2. Low pH inhibited Fe(II) oxidation to produce ROS or Fe(IV), so much less As(III)/Sb(III) were oxidized AMD at pH 2 than those in AMD at pH 3 and 4.

Fe(II) concentration did not significantly affect dissolved total As or Sb concentrations when Fe(II) concentration was 100–500 mg/L (Fig. 3a, d). The generation of As(V) and Sb(V) (Fig. 3c, f) showed that a little of As(III) and Sb(III) were oxidized. Because a little of Fe(II) was oxidized (Fig. S4b), productions of ROS/Fe(IV) and iron oxydroxides were low, so a little of As(III)/Sb(III) be oxidized and adsorbed. The differences of total As/Sb concentrations or dissolved As(III)/Sb(III) concentration were unsignificant in AMD containing 100–500 mg/L Fe(II).

High salinity could inhibit the reaction of H^+ with limestone (Fig. S4c) in AMD containing high Fe(II) concentration, so pH was low in AMD (Fig. S4a). At the same time, low pH suppress Fe(II) oxidation (Fig. S4b) to produce ROS/Fe(IV). The high salinity inhibited Fe(II) oxidation to produce Fe(III) (Millero et al. 1987), which produce acid via hydrolysis reaction. The dissolution of limestone decreased

in AMD containing high Fe(II) concentration (Fig. S3c). So, high Fe(II) concentration can decrease Fe(II) oxidation rate and pH slightly, but low pH can increase production of ROS, so Fe(II) concentration (100–500 mg/L) did not significantly affect oxidation and immobilization of As/Sb.

The concentrations of total As or Sb in AMD with different migration distances increased gradually with the increased of reaction time (Fig. 4a, d). Since limestone is consumed or wrapped by solid phase produced by reactions such as iron (hydr)oxides, resulting in a decrease in the neutralization ability of limestone to AMD. So, the pH of AMD with different flow distances is gradually decreasing. The pH of the tertiary outlet AMD varied slightly and gradually became consistent after 56 h (Fig. S5a). The amount of Fe(II) oxidation decrease gradually with the continuous decreases of pH, resulting in the increasing concentration of Fe(II) in the dissolved state in the AMD (Fig. S5b). Therefore, the production of iron (hydr)oxides decreased, which slows down the growth of adsorption capacity to As/Sb. Overall, the total dissolved of As/Sb increased gradually in the AMD (Fig. 4a, d).
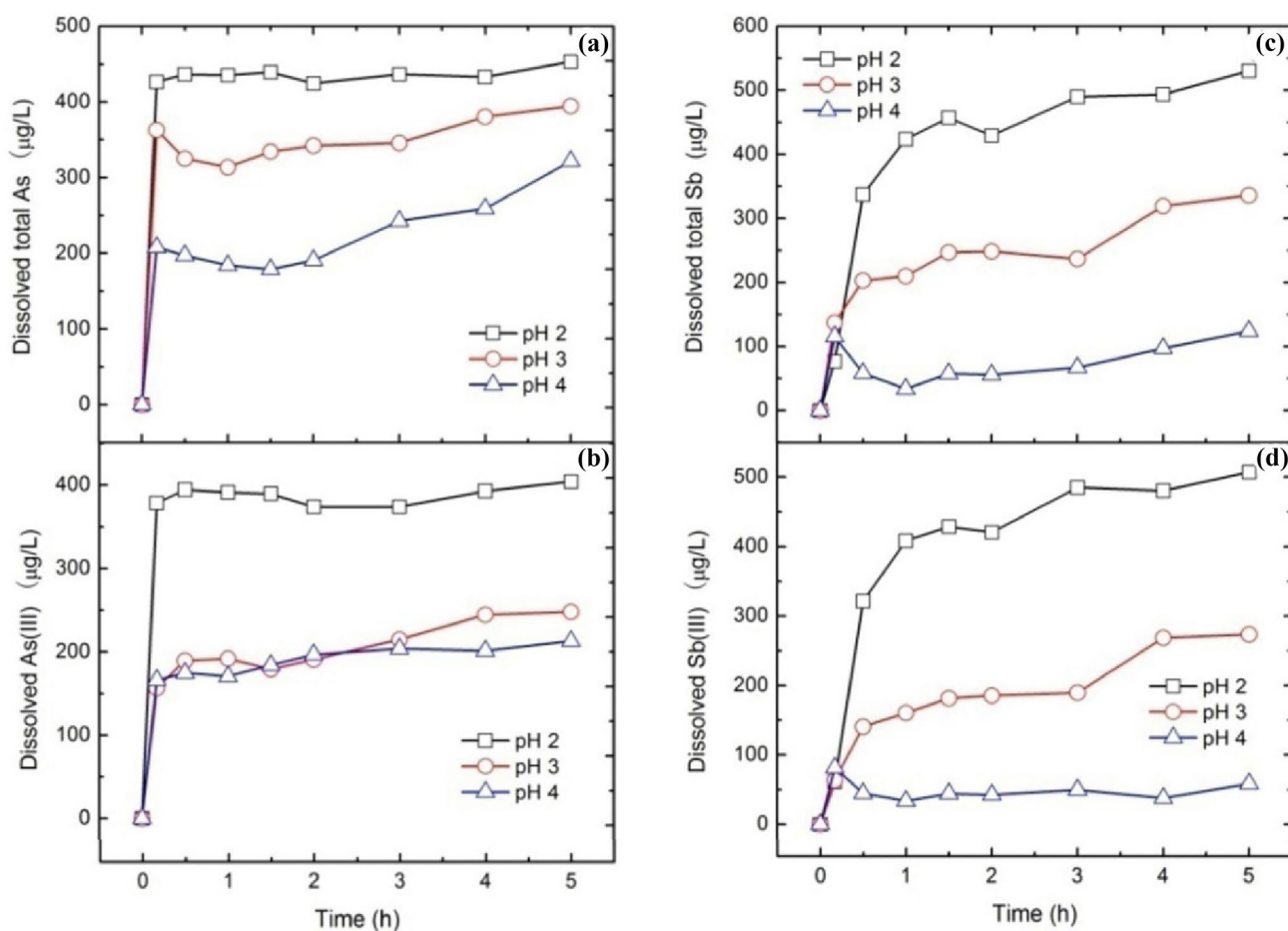
Fig. 2 The concentrations of **a** dissolved total As, **b** dissolved As(III), **c** dissolved total Sb and **d** dissolved Sb(III) in AMD in the third step outlet

The oxidation rate of Fe(II) slowed down with the decrease of pH (Fig. S5b), so the yield of ROS/Fe(IV) produced from oxidation of Fe(II) decreased. The concentrations of dissolved As(III)/Sb(III) increased gradually with reaction time (Fig. 4b, e). Correspondingly, the dissolved As(V)/Sb(V) concentrations showed a decreasing trend (Fig. 4c, f) due to adsorption or coprecipitation of iron (hydr)oxides. It may be that iron (hydr)oxides have a stronger adsorption capacity for Sb than As, so the removeal rate of Sb in the AMD is higher than As.

Fe(II) oxidation driven by carbonatite to produce ROS/Fe(IV) and iron (hydr)oxides in AMD flow (King et al. 1995; Pham and Waite 2008), which facilitated rapid oxidation of As(III)/Sb(III). To evaluate the contribution of ·OH, 2-propanol (100 mM) or ethanol (1 M) was added respectively as an ·OH (Keenan and Sedlak 2008b),or ·OH and Fe(IV) (Shi et al. 2014) scavengers. The results of quenching experiment showed that both of 2-propanol and ethanol had inhibited negligibly oxidation of As(III)/

Sb(III) obviously (Fig. S6). It is possible that As(III)/Sb(III) was adsorbed by iron (hydr)oxides (Amstaetter et al. 2010) and then oxidized by ROS/Fe(IV) which generated mainly on the iron (hydr)oxides (Zhu et al. 2017). The scavengers in solution had not accessed ROS/Fe(IV) well, so 2-propanol or ethanol had not effected the oxidation of As(III)/Sb(III).

Since As(III)/Sb(III) were still rapidly oxidized after the addition of scavengers (Fig. 5), $\cdot O_2^-$ (Ryu and Choi 2004) or H_2O_2 (Leuz and Johnson 2005) produced from Fe(II) oxidation could oxidize a part of As(III)/Sb(III). Fe(II) which was activated by goethite can oxidize As(III) (Amstaetter et al. 2010). Meanwhile, $Fe(OH)_3$ can oxidize Sb(III) also (Belzile et al. 2001). Therefore, oxidation mechanisms of As(III)/Sb(III) in AMD was explored under anoxic condition.

As(III)/Sb(III) can be rapidly oxidized in AMD under anoxic condition, and its oxidation rate increased with the oxygenation time of AMD in the air (Fig. 5). The total Fe(II) concentration in AMD decreased with the increase
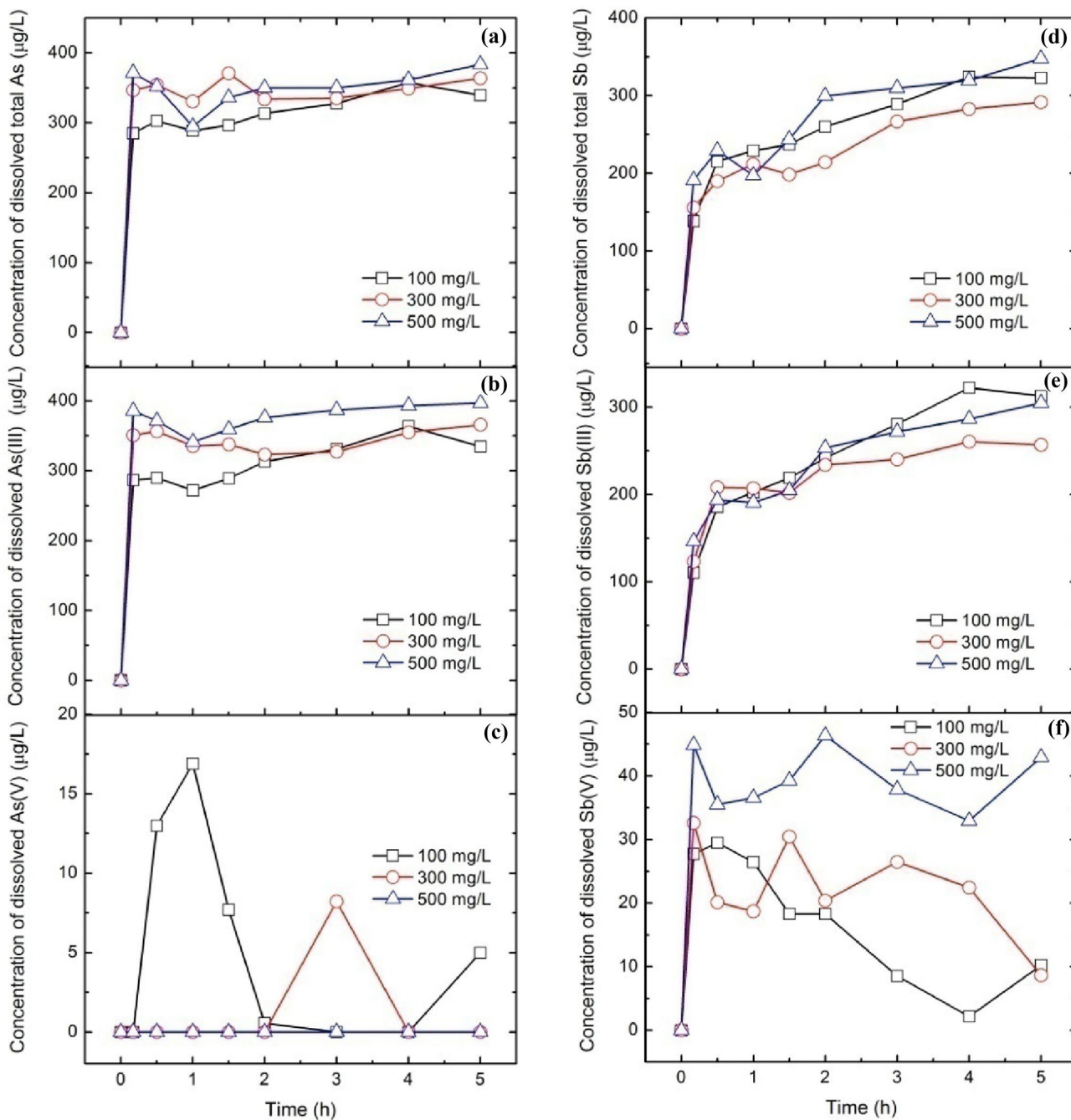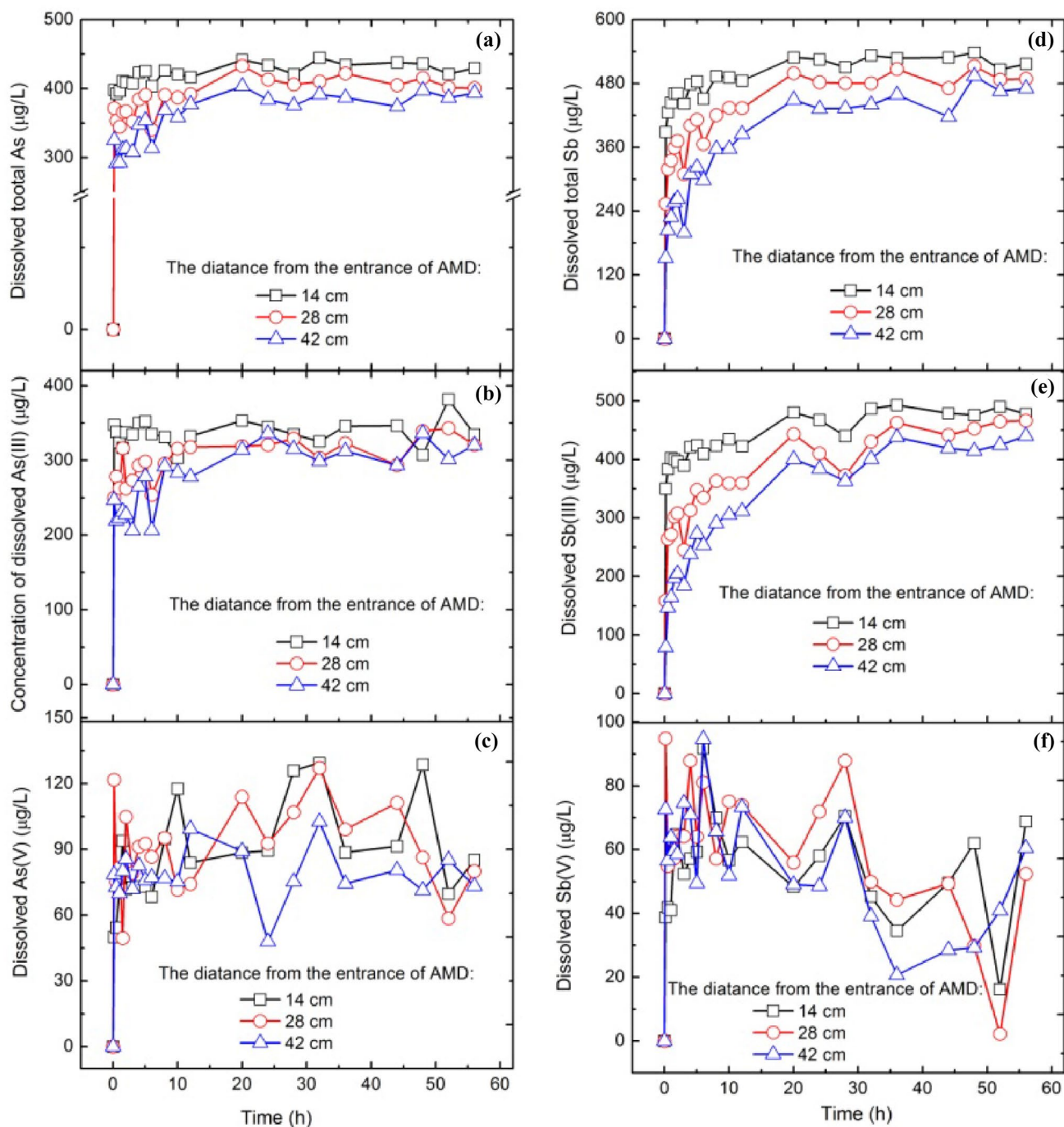
Fig. 3 The concentrations of **a** dissolved total As, **b** dissolved As(III), **c** dissolved As(V), **d** dissolved total Sb, **e** dissolved Sb(III) and **f** dissolved Sb(V) in AMD in the third step outlet

of oxygenation time of AMD (Fig. S8a, b, c). However, there was no significant change in total Fe(II) contents during reaction under anoxic condition (Fig. S8a, b, c). Fe(II) could not be oxidized by O_2 to produce ROS/Fe(IV) to oxidize As(III)/Sb(III) under anoxic condition. Therefore,

ferric (hydr)oxides might be a main oxidant of As(III)/Sb(III). The Fe(II) concentration in AMD with addition of As(III)/Sb(III) was higher than that without addition of As(III)/Sb(III) (Fig. S8a, b, c), indicating that a part of Fe(III) was reduced to Fe(II) by As(III)/Sb(III). Ferric

Fig. 4 The concentrations of **a** dissolved total As, **b** dissolved As(III), **c** dissolved As(V), **d** dissolved total Sb, **e** dissolved Sb(III) and **f** dissolved Sb(V) in AMD in different distance

(hydr)oxides could oxide As(III)/Sb(III) through electron transfer by forming complexes. Sb(III) was oxidized faster in the experiments than that by synthetic iron (hydr)oxides (Belzile et al. 2001). It was possible that Ferric (hydr)oxides could oxide As(III)/Sb(III) through electron

oxides activated by Fe(II) oxidized As(III)/Sb(III) rapidly (Amstaetter et al. 2010). The addition of As(III)/Sb(III) had no obvious effect on the pH of the suspension during the anaerobic oxidation of pollutants (Fig. S8d, e, f).
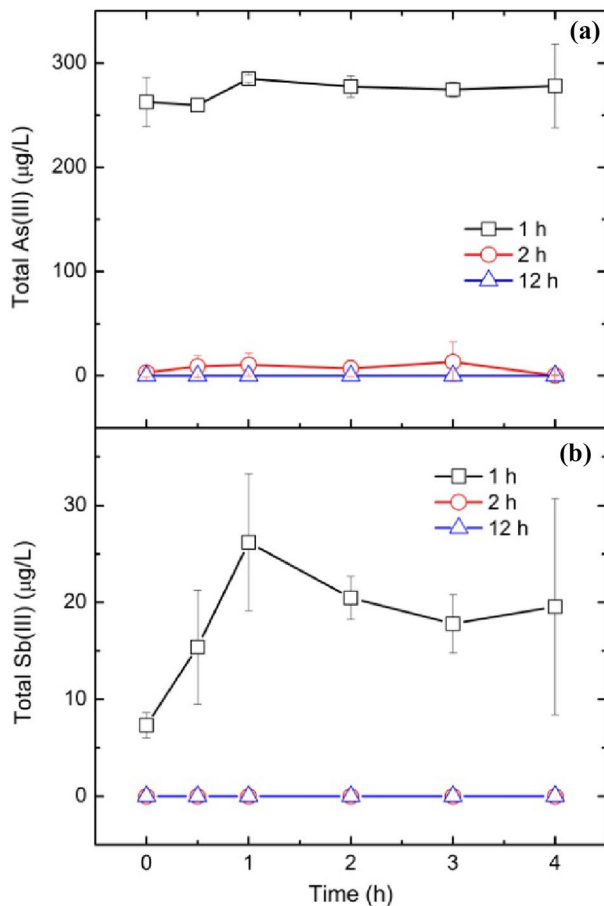
Fig. 5 The concentrations of **a** total As(III), **b** total Sb(III) during anaerobic oxidation of simulated AMD oxidation products

This study investigated the influence of Fe(II) oxidation on the transfer and transformation of As/Sb in simulated AMD induced by carbonate. Low flow and high pH were beneficial for Fe(II) oxidation to produce ROS/Fe(IV) and iron (hydr)oxides to oxidize As(III)/Sb(III). Fe(II) concentration (100–500 mg/L) had negligible influence on oxidation and sediment of As(III)/Sb(III). With increase of reaction time, difference in As(III)/Sb(III), total As/Sb concentrations between different flow distances were decreasing.

References

Amstaetter K, Borch T, Larese-Casanova P, Kappler A (2010) Redox Transformation of Arsenic by Fe(II)-Activated Goethite (α-FeOOH). Environ Sci Technol 44(1):102–108

Arnold T, Baumann N, Krawczyk-Bärsch E, Brockmann S, Zimmermann U, Jenk U, Weiß S (2011) Identification of the uranium speciation in an underground acid mine drainage environment. Geochim Cosmochim Acta 75(8):2200–2212

Belzile N, Chen Y-W, Wang Z (2001) Oxidation of antimony (III) by amorphous iron and manganese oxyhydroxides. Chem Geol 174(4):379–387

Casiot C, Morin G, Juillot F, Bruneel O, Personné J-C, Leblanc M, Duquesne K, Bonnefoy V, Elbaz-Poulichet F (2003) Bacterial immobilization and oxidation of arsenic in acid mine drainage (Carnoulès creek, France). Water Res 37(12):2929–2936

Cheng H, Hu Y, Luo J, Xu B, Zhao J (2009) Geochemical processes controlling fate and transport of arsenic in acid mine drainage (AMD) and natural systems. J Hazard Mater 165(1):13–26

Dixit S, Hering JG (2003) Comparison of arsenic(V) and arsenic(III) sorption onto iron oxide minerals: implications for arsenic mobility. Environ Sci Technol 37(18):4182

Dutta PK, Pehkonen SO, Sharma VK, Ray AK (2005) Photocatalytic Oxidation of Arsenic(III): Evidence of Hydroxyl Radicals. Environ Sci Technol 39(6):1827–1834

Ford D, Williams PD (2013) Karst hydrogeology and geomorphology. Wiley, New York

Guo X, Wu Z, He M, Meng X, Jin X, Qiu N, Zhang J (2014) Adsorption of antimony onto iron oxyhydroxides: adsorption behavior and surface structure. J Hazard Mater 276:339–345

Hug SJ, Leupin O (2003) Iron-catalyzed oxidation of arsenic (III) by oxygen and by hydrogen peroxide: pH-dependent formation of oxidants in the Fenton reaction. Environ Sci Technol 37(12):2734–2742

Jeon B-H, Dempsey BA, Burgos WD (2003) Kinetics and Mechanisms for Reactions of Fe(II) with Iron(III) Oxides. Environ Sci Technol 37(15):3309–3315

Keenan CR, Sedlak DL (2008a) Factors affecting the yield of oxidants from the reaction of manoparticulate zero-valent iron and oxygen. Environ Sci Technol 42(4):1262–1267

Keenan CR, Sedlak DL (2008b) Factors Affecting the Yield of Oxidants from the Reaction of Nanoparticulate Zero-Valent Iron and Oxygen. Environ Sci Technol 42(4):1262–1267

Kiran MG, Pakshirajan K, Das G (2017) Heavy metal removal from multicomponent system by sulfate reducing bacteria: Mechanism and cell surface characterization. J Hazard Mater 324:62–70

Kong L, Hu X, He M (2015) Mechanisms of Sb (III) oxidation by pyrite-induced hydroxyl radicals and hydrogen peroxide. Environ Sci Technol 49(6):3499–3505

Leuz A-K, Johnson CA (2005) Oxidation of Sb (III) to Sb (V) by O_2 and H_2O_2 in aqueous solutions. Geochim Cosmochim Acta 69(5):1165–1172

Millero FJ, Sotolongo S, Izaguirre M (1987) The oxidation kinetics of Fe (II) in seawater. Geochim Cosmochim Acta 51(4):793–801

Razo I, Carrizales L, Castro J, Díaz-Barriga F, Monroy M (2004) Arsenic and heavy metal pollution of soil, water and sediments in a semi-arid climate mining area in Mexico. Water Air Soil Pollut 152(1):129–152

Ryu J, Choi W (2004) Effects of TiO2 surface modifications on photocatalytic oxidation of arsenite: the role of superoxides. Environ Sci Technol 38(10):2928–2933

Shi J, Ai Z, Zhang L (2014) Fe@Fe₂O₃ core-shell nanowires enhanced Fenton oxidation by accelerating the Fe(III)/Fe(II) cycles. Water Res 59:145–153

Stumm W, Lee GF (1961) Oxygenation of Ferrous Iron. Ind Eng Chem 53(20):143–146

Zhou J, Nyirenda MT, Xie L, Li Y, Zhou B, Zhu Y, Liu H (2017) Mine waste acidic potential and distribution of antimony and arsenic in waters of the Xikuangshan mine, China. Appl Geochem 77:52–61

Zhu J, Zhang P, Yuan S, Liao P, Qian A, Liu X, Tong M, Li L (2017) Production of Hydroxyl radicals from oxygenation of simulated AMD due to CaCO₃ -induced pH increase. Water Res 111:118–126